Manuscript

Effects of CCVT Stray Capacitances on Traveling Wave-Based Applications

R. L. A. Reis, F. V. Lopes, W. L. A. Neves, D. Fernandes Jr., and F. G. Almeida Neto

***Abstract*—In this paper, the effects of stray capacitances that may appear on the coupling capacitor voltage transformer (CCVT) during field operation are addressed. Those stray capacitances are usually ignored in the existing limited frequency bandwidth CCVT digital models reported in the literature. A sensitivity analysis is carried out to evaluate how the equipment magnitude and phase frequency responses can be affected when such capacitances are taken into account. Besides, the feasibility of classical CCVT transient response compensators is analyzed in these scenarios. The impact of these features is investigated on the performance of one- and two-ended traveling wave (TW)-based fault location techniques. The obtained results attest that the presence of the stray capacitances improve the performance of two-ended TW-based fault locators, but the classical CCVT compensator may not accurately reproduce the voltage TWs.**

***Keywords*—CCVT, fault location, stray capacitances, transmission lines, traveling waves.**

I. Introduction

THE traveling wave (TW)-based fault locators are typically reported as one of the most robust ways to estimate the short-circuit distance. Although their theoretical basis is quite old [1], the use of these types of techniques have been recently boosted due to technological advancements, such as protective devices presenting sampling rates in the order of MHz. Basically, the existing practical transmission line (TL) TW-based monitoring devices use current [2] and voltage [3] signals as input data.

By using voltage TWs (v_{TWs}) as input data to the TW-based fault locators, the applications are mainly focused on two-ended approaches, as they essentially depend on the detection of the fault-induced incident waves at the TL ends. However, if the subsequent reflected and refracted v_{TWs} are correctly measured, the performance of some TW-based protection functions could be improved, as for instance the directional function, since this process would allow a reliable identification of the forward and backward surges.

It is usually reported in the literature the use of voltage measurements provided by coupling capacitor voltage transformers (CCVTs) in two-ended TW-based fault location (TE-TWFL) applications [4], [5], as well as the benefits of the CCVT frequency response compensation on such routines [6]. Despite the feasibility of using CCVTs to measure the incident fault-induced v_{TWs} [7], [8], due to the increasing number of line TW-based protective devices with higher sampling rates in operation worldwide, there is a need to better understand the equipment performance at higher frequencies, especially in measuring the subsequent reflections and refractions after the initial surge. Such situation is even important to analyze the performance of the classical TW-based fault locators.

However, due to practical limitations, the CCVT frequency response tests are usually limited up to 10 kHz [9], which may not allow a suitable representation of fault-induced high frequencies. As a consequence, the process of estimating the CCVT digital models may not take into account the effects of some stray capacitances along the CCVT circuitry, whose elements may show up in the field during disturbance events. Thus, the CCVT digital models typically present topologies acceptable for the most demanding applications [9], but they may not accurately reproduce the equipment behavior for fault-induced frequencies higher than the referred threshold.

As it is reported that the presence of CCVT stray capacitances may allow the correct detection of the first incident TWs in terms of arrival times [7], [8], [10], most of the analysis and solutions reported in the literature are restricted to the use of such incident TWs. As a consequence, papers that investigate the impact of different stray capacitances on the CCVT responses for frequencies higher than the limited 10 kHz spectrum, as well as on TW-based applications, especially the single-ended ones, are usually not reported. Hence, studies that consider the effects of CCVT stray capacitances on the performance of TW-based functions are attractive to the industry, which may lead to the development of new CCVT models and/or innovative voltage reconstruction strategies.

Therefore, to fulfill this existing gap in the literature and introduce important aspects within the investigation context of the CCVT-induced behavior at higher frequencies, a sensitivity analysis is carried out in this paper considering a 230 kV CCVT digital model reported in the literature, highlighting how different stray capacitances that may appear in real applications (and not included in the CCVT topology) affect its magnitude and phase angle frequency responses. This impact is evaluated on single- and double-ended TW-based fault location techniques. Besides, a CCVT frequency response compensator is implemented to evaluate if the classical methodologies to provide a primary voltage replica is still feasible when such capacitances are present in the equipment circuitry.

To do so, several fault simulations are carried out on a 230 kV transmission network using the Alternative Transients

This work was financed in part by CNPq, Brazil.

R. L. A. Reis and F. G. Almeida Neto are with Federal Rural University of Pernambuco (UFRPE), Brazil (e-mail of corresponding author: raphael.reis@ufrpe.br).

F. V. Lopes is with University of Brasília (UnB), Brazil (e-mail: felipevlopes@unb.br).

W. L. A. Neves and D. Fernandes Jr. are with Federal University of Campina Grande (UFCG), Brazil (e-mail: waneves@dee.ufcg.edu.br and damasio@dee.ufcg.edu.br).

Paper submitted to the International Conference on Power Systems Transients (IPST2021) in Belo Horizonte, Brazil June 6-10, 2021.

Program (ATP) [11], considering the CCVT primary (reference signal), secondary, and compensated secondary measurements as input data to the fault location algorithms. To follow practical procedures [3], voltage waveforms are used as input data in the classical TE-TWFL method. From the obtained results, it is shown that the stray capacitances considerably affect the CCVT frequency responses, which may facilitate the identification of the incident fault-induced TWs on the TE-TWFL routine, but may lead to voltages attenuations and great phase displacements of the subsequent surges in the single-ended approaches. In this way, the classical CCVT compensator may not be effective in reproducing v_{TWs}.

II. Existing CCVT Models

The existing procedures to estimate the CCVT topology and frequency response reported in the literature typically faced some practical limitations, as noise contaminated measurements, difficulties in estimating nonlinear elements, need for data not easily provided by the manufacturer etc. For this reason, the tests have been carried out to provide relatively accurate frequency response measurements up to 10 kHz, which is suitable for studies on the most phasor-based protection applications and electromagnetic transient studies [9].

A typical CCVT circuit topology for a frequency spectrum up to 10 kHz is shown in Fig. 1 by solid lines [9]. For this frequency range, the predominant elements consist in the stack capacitances (C_1 and C_2), the tuning reactor (C_r, R_r and L_r), the step-down transformer (SDT), which is represented by the stray capacitance C_P and the nonlinear magnetic core ($\lambda - i$), the ferroresonance suppression circuit (FSC), and burden, such as a protective device. Basically, the primary voltage (V_{pri}) magnitude is reduced by the stack capacitances to the intermediate point of the SDT, which in turn scales-down such this signal to feed a burden with a secondary voltage (V_{sec}).

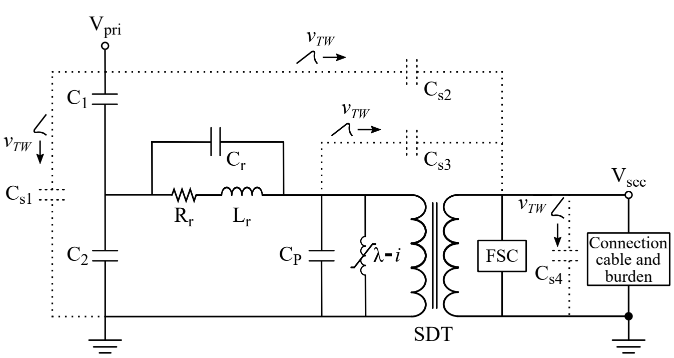

Fig. 1. Typical CCVT circuit topology for electromagnetic transient studies.

With the recent increasing use of TW-based functions, the studies considering the limited frequency bandwidth CCVT models may not reliably represent the equipment performance in the field. Fundamentally, the main concern about the use of voltage signals in TW-based techniques is that the tuning reactor and the SDT may behavior as high impedance paths to the voltage TWs go toward the monitoring device. In fact, the fault-induced high frequency components are almost filtered out by such inductors, in which, together with the other equipment parameters, the CCVT transient and frequency responses may cause attenuated and phase-shifted v_{TWs} to be measured at the secondary terminals.

However, it is possible that other stray capacitances may appear during the equipment operation at high frequencies, as the ones represented by dashed lines in Fig. 1. These capacitances may provide low impedance paths to the v_{TWs} go toward the burden. As a result, although they are not included in most existing CCVT digital models reported in the literature, their presence may affect the equipment transient/frequency responses in the field.

To investigate such scenario, a sensitivity analysis of the magnitude and phase frequency responses of the classical 230 kV/60 Hz CCVT digital model reported in [12] is carried out in this paper. Basically, the stray capacitances C_{s1} through C_{s4} shown in Fig. 1 are inserted in the CCVT circuit, varying their corresponding parameters to verify the impact on the CCVT frequency responses. To do so, typical stray capacitance values were taken into account, such as 600 pF and 8000 pF, as suggested in [1] and [13], respectively. Also, a minimum value of 10 pF was considered to allow comparative analysis.

The CCVT frequency responses were obtained using the ATP *Frequency Scan* routine. Although the CCVT model presents a frequency spectrum up to 10 kHz, the estimated response was simulated up to 1 MHz to analyze the impact of the stray capacitances at higher frequencies, which is within the bandwidth of practical procedures [3]. The obtained CCVT magnitude and phase frequency response dynamics considering the stray capacitances variation are shown in Fig. 2.

As depicted in Fig. 2, the CCVT accuracy is quite acceptable for the most demanding applications at power frequency,

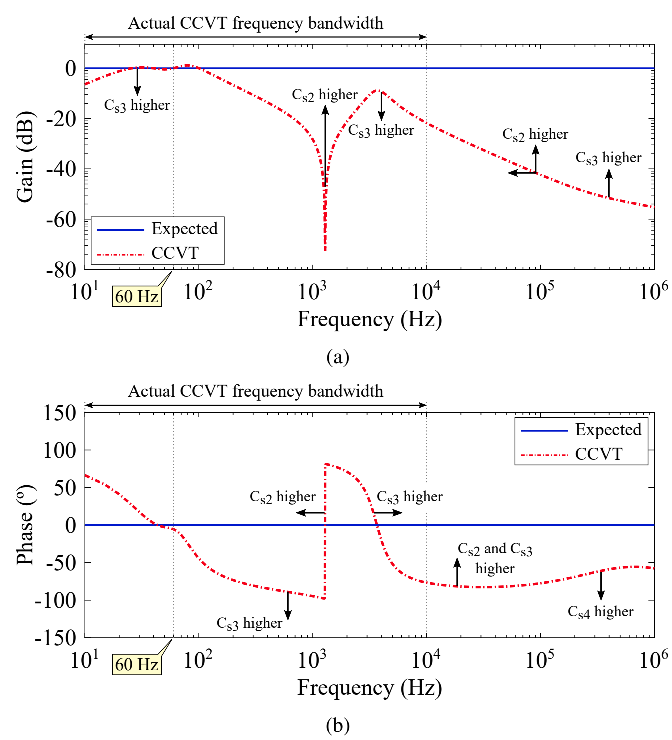

Fig. 2. CCVT frequency response extrapolated up to 1 MHz: (a) magnitude; (b) phase.

since the CCVT secondary signal follows the expected one (primary signal). On the other hand, as long as the stray capacitances are considered in the CCVT circuitry, magnitude and phase angle frequency responses changes are noticeable. Greater impacts are due to C_{s2} and C_{s3}. In fact, these stray capacitances provide direct paths for the v_{TWs} from the equipment primary side to the secondary one. In these cases, besides significantly increasing the CCVT magnitude response at the highest frequencies, a large phase shift is imposed to the voltage signal in such spectrum, in which v_{TW} may lead the expected waveform rather than lag it (the nominal frequency response would lag the expected signal). The C_{s1} did not affect the CCVT frequency responses, whereas C_{s4} imposed a lag phase shift at the highest frequency components, whose element may represent the combined effects of stray capacitances due to the cable used to connect the burden and the FSC.

In this way, as the CCVT magnitude and phase frequency responses are considerably distinct from the nominal ones when the evaluated stray capacitances are considered, the measured v_{TWs} may appear with greater magnitudes and phase shifted, which can jeopardize the TWs polarity analysis. These facts may not be noticed when the limited frequency bandwidth CCVT digital model is considered. Hence, the use of the existing referred CCVT models may not accurately reproduce the TW phenomena on the measured voltage surges.

A. CCVT Compensation Filtering

Classical methodologies to restore an authentic replica of the primary voltage waveform on the CCVT secondary terminals are based on recursive digital filtering processes. Basically, the main purpose of such strategies is designing a filter to reproduce the CCVT inverse transfer function [6], [14]. As a consequence, there is a need to previously know the equipment frequency response to estimate its corresponding transfer function.

In this context, as the typical CCVT digital models reported in the literature present limited frequency bandwidth, these classical filtering strategies may provide accurate compensation in such frequency spectrum. However, their capability in reproducing fault-induced frequencies beyond the existing CCVT model limits are usually not reported in the literature and still need to be evaluated, especially when the stray capacitances shown in Fig. 1 are taken into account.

In order to analyze such scenarios, the CCVT digital recursive filtering compensator reported in [6] was considered. Essentially, the designed digital filter is put in cascade with the CCVT secondary side, in which the CCVT compensated frequency response (CCVT+compensator) is obtained. In Fig. 3, the compensated CCVT frequency response is illustrated and compared with the expected and the CCVT responses, considering the extrapolated frequency range up to 1 MHz. Details about the CCVT transfer function and the filtering design are reported in [6].

As illustrated in Fig. 3, by using the designed compensator, the CCVT-induced high frequency attenuation and phase displacements are significantly reduced in the 10 kHz bandwidth. In fact, as the digital compensator practically reproduces the CCVT inverse transfer function, the corresponding voltage

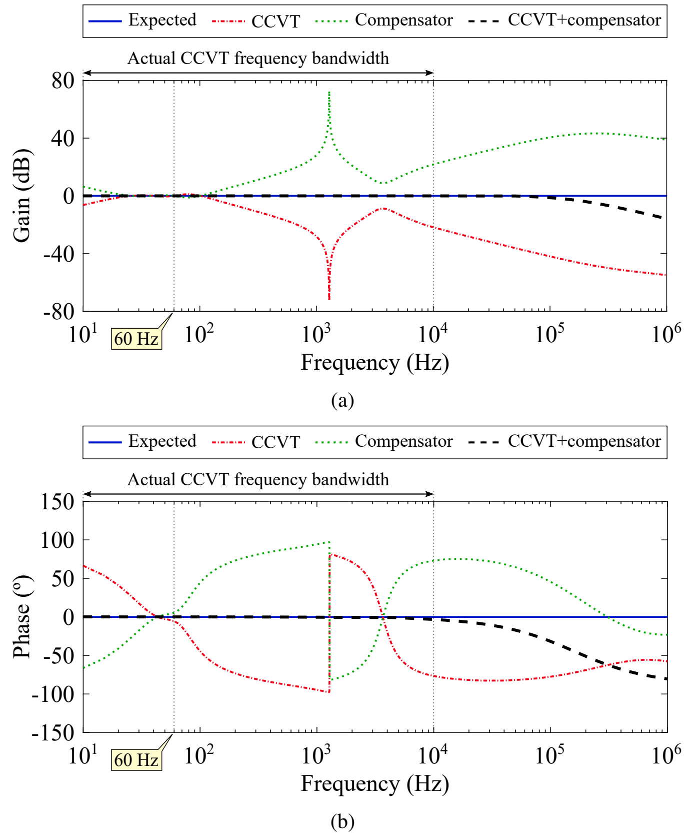

Fig. 3. CCVT frequency response extrapolated up to 1 MHz considering the compensation strategy: (a) magnitude; (b) phase.

output is quite close to the expected signal in such spectrum. However, since it is designed up to 10 kHz, some attenuations and great lag phase shifts can be noticed for frequencies greater than this threshold in the measured voltage signals. These facts may be even more evident if the stray capacitances, as C_{s2} and C_{s3}, are taken into account.

To illustrate such scenarios in time domain, a BC fault, initiated at 90° of the line-to-line voltage, is applied at 10 km away from the monitored bus of the 230 kV/60 Hz system shown in Fig. 4, considering cases with and without C_{s3}. For the cases with C_{s3}, the values of 10 pF and 600 pF were considered. The grid topology is reported in [7], with its parameters adjusted based on actual Brazilian transmission systems.

The expected and the CCVT+compensator waveforms for such fault simulations are presented in Fig. 5(a), and the secondary voltage outputs are shown in Fig. 5(b). To allow comparative analysis, voltage signals are normalized in pu.

As depicted in Fig. 5(b), as greater the C_{s3} value is, the first v_{TWs} are more evident in the CCVT output, whereas higher attenuations are imposed to the subsequent lower frequency oscillations, following the behavior shown in Fig. 2.

Regarding the CCVT compensation strategy, as long as C_{s3} is not considered in the equipment circuitry, its effectiveness is attested since the compensated voltage output follows the expected signal pattern, as presented in Fig. 5(a). However, when C_{s3} is taken into account in the CCVT topology, deviations from the expected waveform are noticed, which become even more evident as greater the C_{s3} is. Indeed, for

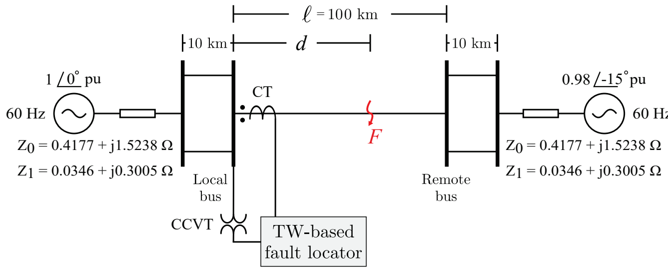

(a)

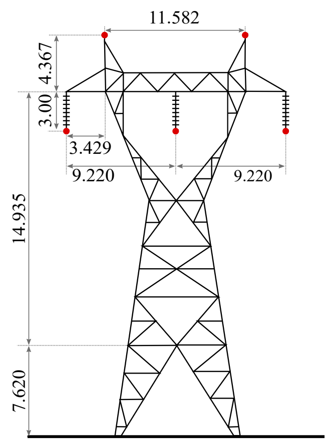

(b)

Fig. 4. 230 kV grid used in the simulations: (a) Single-line diagram; (b) tower structure with distances in meters.

fault-induced frequency components that may be higher than the CCVT limited bandwidth, the designed compensator is not able to accurately reproduce the expected waveform, causing more attenuation and phase shift in the voltage output, whose behavior follows its frequency response illustrated in Fig. 3.

Therefore, the existing limited frequency bandwidth CCVT models are affected by stray capacitances presented along the equipment circuitry, especially those interconnecting the primary and secondary sides. In the same way, the corresponding classical methodologies to restore primary voltage replicas, which are based in such CCVT models, may not be effective at higher frequencies. Such conditions can be even jeopardized if the CCVT aging is considered, since this fact is not usually taken into account during the compensator designing. As a consequence, it is possible that using the existing CCVT digital models and the corresponding compensation strategy during TW-based studies, the field behavior may not be accurately reproduced, since such stray capacitances would be presented.

III. Evaluated TW-Based Methods

In this paper, the classical TE-TWFL and a single-ended correlation-based traveling wave fault location (SEC-TWFL) methods are considered to investigate the impact of CCVT stray capacitances on such routines. The main principles of each technique are presented next.

A. TE-TWFL Technique

The basic principle of the TE-TWFL technique relies on the correct identification of the first fault-induced surges measured at the Local and Remote buses, i.e., the time instants t_{L1} and t_{R1} shown in Fig. 6, respectively. In this way, the short-circuit distance is estimated by $\tilde{d}_2 = \{\ell + (t_{L1} - t_{R1}) \cdot v\}/2$ [15], in which ℓ is the TL length, v is the aerial mode TW propagation speed, and $\tilde{d}_2$ is the estimated fault point. To detect t_{L1} and t_{R1}, the algorithm reported in [16] was used.

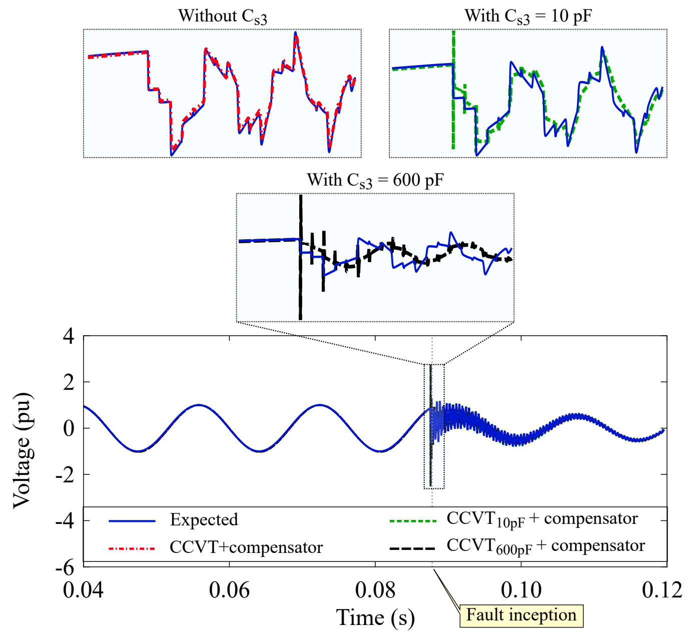

(a)

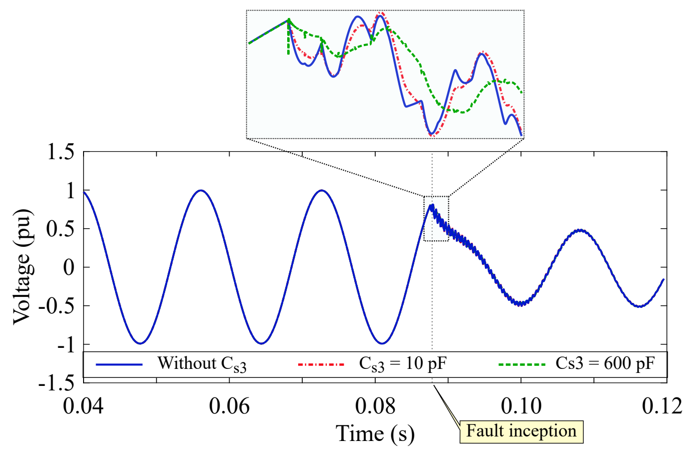

(b)

Fig. 5. Impact of SDT stray capacitances in: (a) the designed digital compensator; (b) secondary measurements.

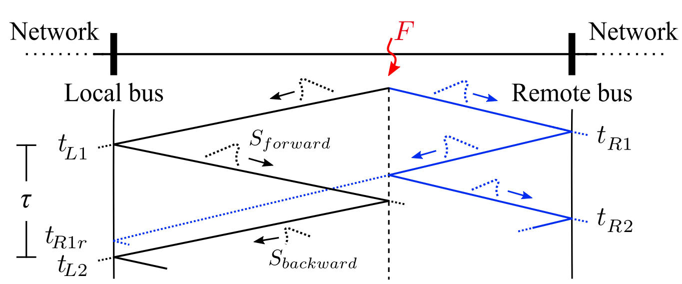

Fig. 6. Fault-induced TWs in an electric power system.

B. SEC-TWFL Techniques

The operating principle of the SEC-TWFL techniques relies on the detection of the time delay between the fault-induced incident and reflected surges, i.e., the time difference between t_{L1} and t_{L2} depicted in Fig. 6, which is represented by τ.

To detect τ, such algorithms separate the TWs measured at the monitored bus into the forward ($S_{forward}$) and backward ($S_{backward}$) TW relaying signals. Fundamentally, these waveforms are computed considering the general solutions of the lossless TL partial differential equations, which are:

$$v(x,t) = f_1(x - \upsilon t) + f_2(x + \upsilon t), \tag{1}$$

$$i(x,t) = \frac{1}{Z_s}\left[f_1(x - \upsilon t) - f_2(x + \upsilon t)\right], \tag{2}$$

where Z_s is the surge impedance, f_1 and f_2 represent the surges traveling in the forward and backward direction, respectively [1].

Thus, by performing the $v + Z_s i$ and $v - Z_s i$ operations in (1) and (2), the $S_{forward}$ and $S_{backward}$ signals are obtained. Since the fault-induced reflected waves present substantially the same wave shapes as the incident surges [17], a correlation function may be used to detect the similarities between these TWs. As a consequence, a maximum positive peak in the correlation function output is expected when $S_{forward}$ and $S_{backward}$ are matched, whose the corresponding time delay τ can be used to estimate the short-circuit distance, as $\tilde{d}_1 = (\upsilon \cdot \tau \cdot \Delta t)/2$ [15], being Δt the sampling period, and $\tilde{d}_1$ the estimated fault point.

IV. TW-Based Fault Location Methods Performance Tests

In order to evaluate the impact of the CCVT stray capacitances that may appear in the field on the TW-based fault locators, the C_{s3} is considered in the subsequent tests, assuming the 10 pF and 600 pF values. Also, the feasibility of the CCVT compensator is investigated on these techniques when such capacitances are taken into account.

Considering the power grid presented in Fig. 4, the faults were applied at d km away from the Local bus on the 100 km long TL, assuming the JMarti frequency-dependent model, and a sampling frequency of 1 MHz. The TW propagation speed υ was determined by a TL energization maneuver, which resulted in approximately 298.863 km/s.

During the simulation studies, the primary, CCVT and CCVT+compensator measured voltages are used as input data to estimate $\tilde{d}_1$. To follow practical applications [3], these data are also considered to estimate $\tilde{d}_2$. To allow comparative analysis with the most traditional procedures, current data are also taken into account to compute $\tilde{d}_2$. Since the main purpose here is investigating the impact of additional stray capacitances on the v_{TW} measurements provided by the limited frequency bandwidth CCVT, noise-free fault scenarios are carried out. Besides, to minimize the effects of mixing mode phenomena and possible refracted waves overlapping the reflected surges, only ungrounded faults are considered.

Basically, 40 fault simulations are carried out for each considered input data, varying the short-circuit parameters, such as type, resistance, inception angle and location, resulting in a total amount of 280 evaluated scenarios. The simulation variables are shown in Table I. In each simulation, the absolute percentage error is computed as $\varepsilon = (|d - \tilde{d}|/\ell) \cdot 100\%$, being d the actual fault point.

TABLE I
FAULT PARAMETERS USED IN THE ATP SIMULATIONS

Simulation variables	Values
Fault location (km)	10, 30, 50, 70, 90
Fault type	BC, ABC
Inception angle (°)	0, 90
Fault resistance (Ω)	1, 50

The estimated ε results for each evaluated method are shown in Fig. 7 as boxplots, considering an error threshold for acceptable estimations as about three tower spans (approximately 1 km) in this paper. In this way, the statistic errors presented as boxplots take into account only the cases in which the errors are smaller than 1 km. For errors greater than this threshold, it is considered that the fault location methods did not converge. The number of converging cases for each input data is illustrated as bar graphs right after the corresponding boxplot, considering the right y-axis.

From the obtained results presented in Fig. 7, the best estimations were provided by the TE-TWFL method, as expected since it only depends on the identification of the first incident TWs at both TL ends. In this context, although the technique has not converged in 1 case when CCVT secondary voltages are used as input data, such error was smaller than 2 km. The performance of the TE-TWFL routine was even improved when the combined effect of C_{s3} and C_{s4} was considered in the CCVT topology. As a result, the presence of stray capacitances that may appear in the field could enhance the identification of such TWs. These obtained results indicate the feasibility in using voltage signals when just the first incident surges are required in the TW-based application, especially because its performance was similar to the one considering current measurements as input data.

Regarding the SEC-TWFL method, the worst scenarios were obtained by using the CCVT measurements, in which the technique has not converged in 36 cases out of 40. In fact, the CCVT-induced magnitude attenuation and phase displacement have significantly affected the algorithm performance and reliability. Such characteristic is more noticeable when C_{s3} and C_{s4} are considered, when the obtained maximum error is even higher than the case without such stray capacitances.

However, by using the compensator, greater maximum errors were obtained when C_{s3} was presented in the equipment circuitry. Indeed, since the filtering strategy is designed to restore a limited CCVT frequency bandwidth, the presence of other stray capacitances has led to a CCVT frequency response changing, which have affected the compensator accuracy. This feature may be even jeopardized if the CCVT aging is considered. As a consequence, unless more wide-ranging frequency tests are carried out to estimate the equipment frequency response, the use of such compensators may be limited in field applications or it needs to be redesigned.

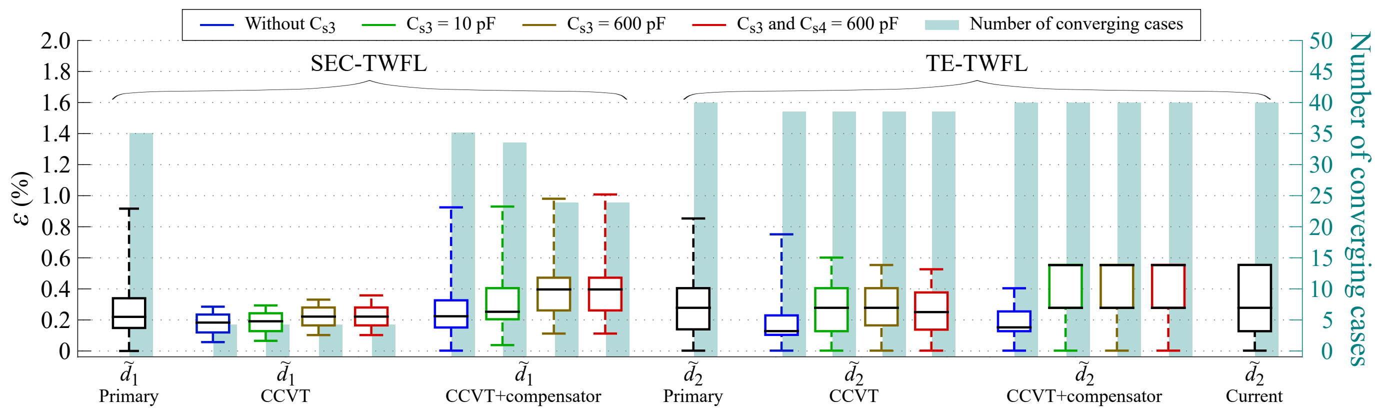

Fig. 7. Boxplots representing the absolute percentage errors for the SEC-TWFL and TE-TWFL methods.

Therefore, the presence of other stray capacitances in the CCVT circuitry, such as C_{s3}, affects the measured v_{TWs}, which can provide a low impedance path for the first fault-induced TWs to be detected at the equipment secondary terminals, but can even provide more attenuations and phase shift for the damped subsequent surges. As a result, the existing CCVT digital models reported in the literature may limit accurate TW representations, which highlights the need of CCVT models that consider such elements. It is worth mentioning that, although the obtained results still need tests with real apparatus, they can be considered as a starting point to clarify a subject scarcely reported in the literature.

V. Conclusions

In this paper, the effects of different stray capacitances that may appear in the CCVT circuitry during field operation are addressed, pointing out the limitation of the existing CCVT digital models reported in the literature in allowing accurate TW evaluations. To do so, a sensitivity analysis was carried out in a 230 kV CCVT model to verify its frequency response changing when such stray capacitances are considered. Besides, a recursive filtering strategy to compensate the CCVT frequency response was also considered. The impact of these features was evaluated on SEC- and TE-TWFL functions.

From the obtained results, the existing limited frequency bandwidth CCVT digital models may not accurately reproduce v_{TWs}, especially the subsequent reflected surges. The greater impact was due to the stray capacitances that interconnect the equipment primary and secondary sides, which has led to amplifications in the first fault-induced waves and phase shifts, although such components presented in the secondary side, as near FSC, also has caused phase displacements. As a consequence, the reliability of the classical compensators that are designed to reproduce the CCVT inverse frequency response in its corresponding limited bandwidth is affected by such elements, and its use may be limited in TW applications.

The presence of such capacitances has not improved the correct identification of the reflected surges in the SEC-TWFL performance evaluations, although such feature has facilitated the detection of the first fault-induced incident TWs, improving the performance of the TE-TWFL method.

References

[1] A. Greenwood, *Electrical Transients in Power Systems*. New York, NY - USA: Wiley-Interscience, 1991.
[2] *SEL-T400L: Instruction manual*, Schweitzer Engineering Laboratories, Washington, USA.
[3] *Reason RPV311: Technical manual*, GE Grid Solutions, Norwalk, USA.
[4] R. L. A. Reis, W. L. A. Neves, and D. Fernandes Jr., “Influence of instrument transformers and anti-aliasing filters on the performance of fault locators,” *Electric Power Systems Research*, vol. 162, pp. 142 – 149, 2018.
[5] R. L. A. Reis, W. L. A. Neves, F. V. Lopes, and D. Fernandes Jr., “Coupling capacitor voltage transformers models and impacts on electric power systems: A review,” *IEEE Transactions on Power Delivery*, vol. 34, no. 5, pp. 1874–1884, Oct 2019.
[6] R. G. Bainy, F. V. Lopes, and W. L. A. Neves, “Benefits of CCVT secondary voltage compensation on traveling wave-based fault locators,” in *2014 IEEE PES General Meeting | Conference Exposition*, July 2014, pp. 1–5.
[7] A. Guzmán, B. Kasztenny, Y. Tong, and M. V. Mynam, “Accurate and economical traveling-wave fault locating without communications,” in *2018 71st Annual Conference for Protective Relay Engineers (CPRE)*, March 2018, pp. 1–18.
[8] E. O. Schweitzer, B. Kasztenny, and M. V. Mynam, “Performance of time-domain line protection elements on real-world faults,” in *2016 69th Annual Conference for Protective Relay Engineers (CPRE)*, 2016, pp. 1–17.
[9] D. Fernandes Jr., W. Neves, and J. Vasconcelos, “Coupling capacitor voltage transformer: A model for electromagnetic transient studies,” *Electric Power Systems Research*, vol. 77, no. 2, pp. 125 – 134, 2007.
[10] A. Guzmán, M. V. Mynam, V. Skendzic, and J. L. Eternod, “Directional elements - how fast can they be?” in *72nd Annual Georgia Tech Protective Relaying Conference*, May 2018, pp. 1–16.
[11] *ATP - Alternative Transient Program*, Leuven EMTP Center, Herverlee, Belgium, 1987.
[12] *EMTP Reference Models for Transmission Line Relay Testing*, IEEE Power System Relaying Committee, 2004. [Online]. Available: http://www.pes-psrc.org
[13] “IEEE application guide for transient recovery voltage for ac high-voltage circuit breakers,” *IEEE Std C37.011-2005 (Revision of IEEE Std C37.011-1994)*, pp. 1–72, 2006.
[14] E. P. Machado, D. Fernandes, and W. L. A. Neves, “Tuning CCVT frequency response data for improvement of numerical distance protection,” *IEEE Transactions on Power Delivery*, vol. 33, no. 3, pp. 1062–1070, June 2018.
[15] P. F. Gale, P. A. Crossley, X. Bingyin, G. Yaozhong, B. J. Cory, and J. R. G. Barker, “Fault location based on travelling waves,” in *Developments in Power System Protection, 1993., Fifth International Conference on*, 1993, pp. 54–59.
[16] F. V. Lopes, D. Fernandes Jr., and W. Neves, “A traveling-wave detection method based on park’s transformation for fault locators,” *IEEE Transactions on Power Delivery*, vol. 28, no. 3, pp. 1626–1634, 2013.
[17] P. A. Crossley and P. G. McLaren, “Distance protection based on travelling waves,” *IEEE Transactions on Power Apparatus and Systems*, vol. PAS-102, no. 9, pp. 2971–2983, Sep. 1983.